Acta Crystallographica Section D
Biological Crystallography
ISSN 0907-4449

The structure of greylag goose oxy haemoglobin: the roles of four mutations compared with bar-headed goose haemoglobin

Yu-He Liang, Xiao-Zhou Liu, Shun-He Liu† and Guang-Ying Lu*

National Laboratory of Protein Engineering and Plant Genetic Engineering, College of Life Sciences, Peking University, Beijing 100871, People's Repbulic of China

† Present address: Department of Biochemistry, Case Western Reserve University, Cleveland, Ohio 44106-4935, USA.

Correspondence e-mail: lugy@pku.edu.cn

Received 3 May 2001
Accepted 4 October 2001

PDB Reference: greylag goose oxy haemoglobin, 1faw.

The greylag goose (*Anser anser*), which lives on lowlands and cannot tolerate hypoxic conditions, presents a striking contrast to its close relative the bar-headed goose (*A. indicus*), which lives at high altitude and possesses high-altitude hypoxia adaptation. There are only four amino-acid residue differences at α18, α63, α119 and β125 between the haemoglobins of the two species. The crystal structure of greylag goose oxy haemoglobin was determined at 3.09 Å resolution. Its quaternary structure is slightly different from that of the bar-headed goose oxy haemoglobin, with a rotation of 2.8° in relative orientation of the two dimers. Of the four mutations, those at α119 and β125 produce contact changes in the $\alpha_1\beta_1$ interface and may be responsible for the differences in intrinsic oxygen affinity between the two species; those at α18 and α63 may be responsible for the differences in quaternary structure between the two species.

1. Introduction

Greylag geese live in Europe and continental Asia. In China, they live and breed in northern China and migrate annually to southern China at the end of autumn. They cannot tolerate hypoxia (Swan, 1970) and present a striking contrast to their closest highland relative, the bar-headed goose (*A. indicus*). Bar-headed geese live in the Qinghai Lake area in China at an altitude of 4000–6000 m and migrate annually to India over the Himalayas (~9000 m altitude) in late autumn. They can tolerate high-altitude hypoxia and even short exposure at 10 700 m (Black & Tenny, 1980).

Previous research indicated that the bar-headed goose haemoglobin (Hb) possesses a slightly higher intrinsic oxygen affinity than the greylag goose Hb (Petschow *et al.*, 1977). There are only four differing residues between the major component HbA of the Hbs of the two species, at the positions α18(A16), α63(E12), α119(H2) and β125(H3). They are Gly, Ala, Pro and Glu for greylag goose Hb (Braunitzer & Oberthur, 1979) and Ser, Val, Ala and Asp for bar-headed goose Hb (Oberthur *et al.*, 1980), respectively. Previous research predicted that α18 is an external residue, α63 is in a surface crevice and that a hydrophilic side chain of β125(H3) would protrude into the surrounding water (Fermi & Perutz, 1981), none of which is likely to affect function. Therefore, it was postulated that the mutation Proα119Ala alone is responsible for the high intrinsic oxygen affinity of the bar-headed goose Hb. The substitution by Ala causes the loss of a van der Waals contact between Proα119(H2) and Leuβ55(D6) at the $\alpha_1\beta_1$ interface which exists in the greylag goose Hb. Any gap loosening the $\alpha_1\beta_1$ interface and relaxing the deoxy or T (tense) structure makes the T state with low oxygen affinity

unstable and facilitates transfer from the T state to the R (relaxed) state with high oxygen affinity (Oberthur *et al.*, 1982; Perutz, 1983; Perutz *et al.*, 1987; Hiebl *et al.*, 1987). Site-directed mutagenesis at α119 and β55 in human Hb (Jessen *et al.*, 1991; Weber *et al.*, 1993) and the crystal structure of bar-headed goose oxy Hb (Zhang *et al.*, 1996) support this postulation.

Only two avian Hb structures, bar-headed goose [oxy Hb (Zhang *et al.*, 1996); met Hb (Liu *et al.*, 2001)] and chicken (oxy HbD, which is the minor component of adult chicken Hb; Knapp *et al.*, 1999), have been solved so far. There is no direct structural evidence from greylag goose Hb. In the present work, the structure of greylag goose oxy Hb, the third structure of an avian Hb species, is reported and compared with the known structure of bar-headed goose oxy Hb (Zhang *et al.*, 1996), which not only determines whether the contact of α119 with β55 does exist in greylag goose Hb, but also provides information about whether the other three residues which differ between the two species are functionally neutral as predicted previously.

2. Materials and methods

2.1. Crystallization and data collection

Blood drawn from the vein of a greylag goose was added to an equal volume of 2.5% sodium citrate in 0.82% NaCl solution and centrifuged at 2500 rev min^{-1} for 10–15 min. The red cells were washed two or three times with 0.82% NaCl solution and then lysed with an equal volume of distilled water. Cell membrane and other insoluble materials were removed by adding half a volume of CCl_4, shaking the mixture and then centrifuging at 4000 rev min^{-1} for 20 min. The haemolytic solution was thoroughly dialyzed against distilled water and concentrated to about 60 mg ml^{-1}. Crystallization was carried out by the hanging-drop vapour-diffusion method at 291 K. A 10 µl droplet containing 25–30 mg ml^{-1} Hb, 7% PEG 6000 and 70 m*M* potassium phosphate buffer pH 6.8 was equilibrated against 1 ml reservoir solution consisting of 14–17% PEG 6000 in the same buffer. Crystals were obtained with maximum dimensions of 0.5 × 0.6 × 0.2 mm within 7–10 d. Data were collected on a MAR Research IP area detector using Cu $K\alpha$ radiation (λ = 1.5418 Å) from a Rigaku RU-200–1 rotating-anode X-ray generator operating at 50 kV, 70 mA and 291 K. The crystal-to-detector distance was 150 mm. A total of 100 frames were collected with an interval of 1.5° and 8 min per frame. The data were processed with program *DENZO* and *SCALEPACK* (Howard *et al.*, 1987). The crystal belongs to the monoclinic space group $P2_1$, with unit-cell parameters a = 57.55, b = 80.62, c = 72.57 Å, β = 102.75°. There is one Hb tetramer molecule in each asymmetric unit, with a V_M of 2.53 Å^3 Da^{-1}. A total of 56 170 observations of 12 746 independent reflections within the resolution range 31.3–3.09 Å were collected with an R_{merge} of 11.3% and a completeness of 96.4%. For the highest resolution shell (3.10–3.2 Å) the completeness is 95.2%. The data collection and unit-cell parameters are summarized in Table 1.

Table 1
Crystallographic data statistics of the greylag goose oxy Hb.

A.u., asymmetric unit. Values in parentheses are for the highest resolution shell.

Space group	$P2_1$
Unit-cell parameters (Å, °)	a = 57.55, b = 80.62, c = 72.57, β = 102.75
No. of molecules in a.u.	1
No. of observations	56170
No. of unique reflections	12746
Resolution (Å)	3.09 (3.10–3.20)
Completeness of data (%)	96.4 (95.2)
Multiplicity	4.4 (2.7)
R_{merge}† (%)	11.3 (33.4)

† $R_{merge} = \sum_h \sum_i |I_i - \langle I \rangle| / \sum_h \sum_i I_i$, where I_i is the measured intensity for reflection i and $\langle I \rangle$ is the mean intensity.

2.2. Structure determination and refinement

The structure was solved by molecular-replacement methods using *X-PLOR* 3.851 (Brünger, 1992). The dimer of the bar-headed goose oxy Hb structure at 2.0 Å resolution (PDB code 1a4f; Zhang *et al.*, 1996) was used to produce a tetramer by an operation of the crystallographic twofold axis. The resulting tetramer was used as search model, as there is one Hb tetramer molecule in an asymmetric unit of the greylag goose oxy Hb structure. The rotation-function calculation was carried out using the data within the resolution range 10–3.09 Å. Two remarkable peaks were obtained at (ψ = 0.855, φ = 60.000, χ = 268.855°) and (181.145, 60.000, 269.145°), respectively. The two peaks show a difference of 180° in ψ, indicating that they are related by an intramolecular non-crystallographic twofold axis and they are hence equivalent. The first peak was taken for translation-function calculation using the data within the resolution range 8–3.09 Å. A highest peak was found at translation vectors Δx = 5.340, Δy = 0.000 and Δz = 3.623 Å, with a peak height of 1.35 times as that of the next highest peak. After rigid-body refinement the R factor is 0.29 and the correlation coefficient is 0.766. The molecular packing in the unit cell is plausible. The four residues of the search model were replaced by those of greylag goose Hb. Structure refinement was performed with *CNS* (Brunger *et al.*, 1998). The structure model was fitted to the electron-density map by manual adjustment using *XFIT* (McRee, 1992) between each round of refinements. Since the ratio of data to free dimension parameters is low (0.83) at the resolution of 3.09 Å using a tetramer as model, in order to raise the ratio and the reliability of the refinement only the coordinates of half a molecule, *i.e.* one $\alpha\beta$ dimer, were used as independent parameters in the refinements; the coordinates of another dimer had the same parameters of the first dimer but were related by the strict non-crystallographic twofold axis. In this way, the ratio of data to free dimension parameters was raised twofold. The dimer model consisting of total 2325 non-H atoms from 287 residues, two haem groups and two oxygen molecules was refined using all 11 543 reflections within the resolution range 31.3–3.09 Å, in which data completeness is 96.4%. 10 521 of 11 543 reflections were used as the working set and 1022 (8.5%) as a test set for monitoring

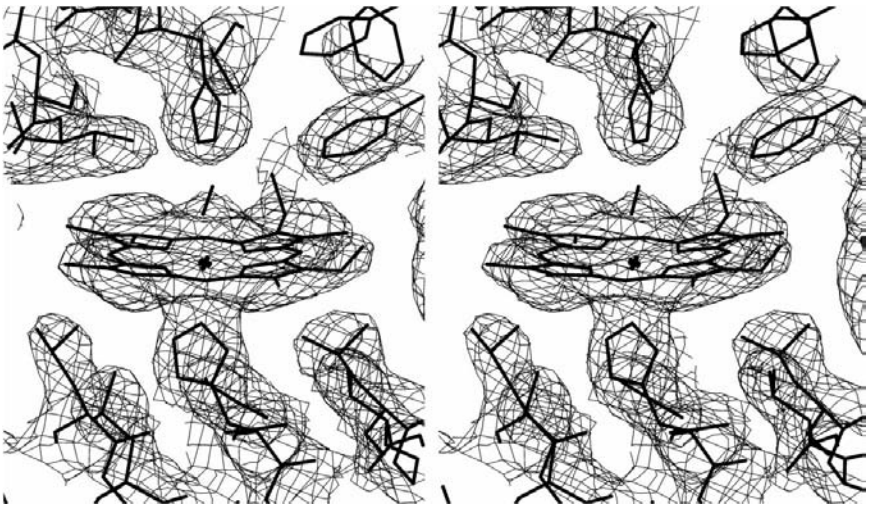

Figure 1
$2mF_o - DF_c$ electron-density map around haem group in the α-subunit of greylag goose oxy Hb.

Table 2
Refinement results of greylag goose oxy Hb structure.

R factor (%)	17.4
R_{free} (%)	21.9
Resolution range (Å)	31.3–3.09
No. of reflections	11543
Final refined model	
Number of protein non-H atoms	2235
Number of heterogen atoms	90
R.m.s. deviation from ideality	
Bond distances (Å)	0.007
Bond angles (°)	1.60
Dihedral angles (°)	19.5
Improper angles (°)	1.15
Average *B* factor (Å^2)	
Total	29.7
Main-chain atoms	26.8
Side-chain atoms	32.5
Ramachandran plot	
Most favourable regions (%)	87.9
Additional allowed regions (%)	11.3
Generously allowed regions (%)	0.8
Disallowed regions (%)	0.0

the progress of the refinements and the validation of the structural model. Before each cycle of *CNS* refinement, rigid-body refinement was performed on the resulting tetramer to obtain the exact non-crystallographic symmetric parameters (the rotation matrix and the translation vectors) and finally the resulting $\alpha\beta$ dimer was deleted. Slow-cool annealing protocol refinements (Brunger *et al.*, 1998) were carried out against a maximum-likelihood target with starting temperature of 5000 K and a final temperature of 300 K with a cooling rate of 25 K per cycle. Group *B*-factor refinement was then used to refine the model. In each refinement step, initial anisotropic overall *B*-factor correction with a lower resolution limit of 6 Å and bulk-solvent correction were applied to the data. The model was harmonically restrained during the slow-cool annealing refinements with energy constants of 42 kJ mol^{-1} Å^2 for all C^α atoms. After each refinement cycle, σ_A-weighted $2mF_o - DF_c$ and $mF_o - DF_c$ maps were calculated and manual adjustments of the model were performed. The refinements resulted in a final *R* factor of 0.174 and an R_{free} factor of 0.219. The density level of the bulk-solvent model is 0.309 e Å^{-3} and its *B* factor is 27.1 Å^2. The water molecules were not added to the model as the resolution is not sufficiently high. The results of the refinements are summarized in Table 2.

2.3. Structure analysis and comparison

The r.m.s. deviations between the structures of the greylag goose oxy Hb and the bar-headed goose oxy Hb (Zhang *et al.*, 1996) were calculated using *XTALVIEW* (McRee, 1992). The planarity of the haem was calculated using *GEOMCALC* from the *CCP*4 suite (Collaborative Computational Project, Number 4, 1994). The BGH fitting frame defined by Baldwin & Chothia (1979) was used for comparison of different human Hb froms, in which the $\alpha_1\beta_1$ contact interface was used as the reference region. The Zhang fitting frame defined by Zhang *et al.* (1996) was used for comparison between avian Hb and human Hb, since structural differences between avian and human Hbs make the region used by the BGH frame less suitable for overlapping the coordinates. In the Zhang frame, the fitting residues are α3–13, α31–42, α54–73, α80–84, α97–104, α117–136, β26–37, β62–68, β106–114 and β127–139, with a total of 117 amino-acid residues and 468 atoms. These account for 40.8% of the main-chain atoms in the $\alpha\beta$ dimer. The contacts between subunits and quaternary geometries of tetramers were calculated using *CNS* (Brunger *et al.*, 1998). The adopted criteria for van der Waals contacting distances are C—C, 4.1 Å; C—N, 3.8 Å; C—O, 3.7 Å; N—N, 3.4 Å; N—O, 3.4 Å; O—O, 3.3 Å (Acqua *et al.*, 1998).

3. Results

3.1. The quality of the structure

The quality of the final $\alpha\beta$-dimer structure excluding H atoms and water molecules in half an asymmetric unit is summarized in Table 2. The structure contains 2235 non-H protein atoms and 90 heterogen atoms which fit well to the $2mF_o - DF_c$ electron-density map. An example electron-density map is shown in Fig. 1 for the region around the α haem group. The stereochemical quality of the structure as assessed by *PROCHECK* (Laskowski *et al.*, 1993) is excellent. The coordinate error evaluated by a Luzzati plot (Luzzati, 1952) is 0.37 Å.

3.2. Subunit structure and quaternary structure

The overall structure of greylag goose oxy Hb superimposes well with that of bar-headed goose oxy Hb (1a4f; Zhang *et al.*, 1996). The overall tertiary and quaternary structures of the greylag goose oxy Hb are similar to but slightly different from

those of the bar-headed goose oxy Hb. The C^{α} traces of the two Hbs fit well to each other, but the difference between the α-subunits of the two species is larger than that between the β-subunits (Fig. 2). The r.m.s. deviations between the α-subunits, β-subunits, $\alpha\beta$ dimers and tetramers are 0.5218, 0.4304, 0.4917 and 0.5900 Å, respectively. Since there are only four residue differences between the two Hbs and three of them are in the α-subunit, this must be the reason why the deviation between their α-subunits is larger than that between their β-subunits.

Table 3
Comparison of relative rotation and translation between $\alpha_1\beta_1$ and $\alpha_2\beta_2$ dimers.

B-G, bar-headed goose; G-G, greylag goose; C-D, chicken HbD.

Oxy Hbs	Human		B-G		G-G	
	Rot. (°)	Trans. (Å)	Rot. (°)	Trans. (Å)	Rot. (°)	Trans. (Å)
B-G	4.3	1.3				
G-G	1.6	1.3	2.8	0.5		
C-D	1.5	0.8	3.1	0.2	0.4	0.1

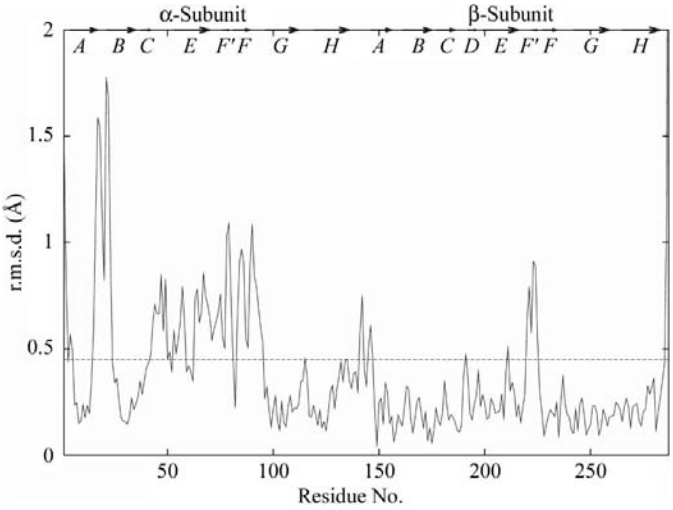

Figure 2
Plot of the r.m.s. deviations between the main-chain atoms of greylag goose and bar-headed goose oxy Hbs as a function of the residue number for the α-chain (1–141) and β-chain (142–287). The dashed horizontal line shows twice the r.m.s. deviation of the BGH fitting frame.

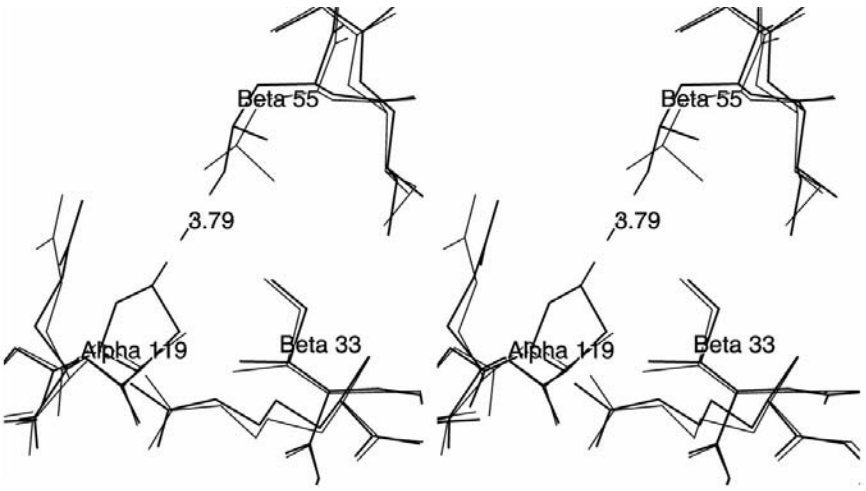

Figure 3
Contact between Proα119(H2) and Leuβ55(D6) in greylag goose oxy Hb (thick line). In bar-headed goose oxy Hb (thin line) Alaα119 does not contact Leuβ55.

The quaternary structural differences of Hbs can be characterized by the rotation angle and the translation between the two dimers in a Hb tetramer molecule. To study the quaternary structure differences between greylag goose oxy Hb and bar-headed goose oxy Hb, comparisons of the relative rotation and translation between the two dimers among in oxy Hbs were performed (Table 3). The conclusion can be drawn that the quaternary structure of the greylag goose oxy Hb (and chicken oxy HbD) is similar to the typical R state of the human oxy Hb and is different from that of the bar-headed goose oxy Hb. In other words, the bar-headed goose oxy Hb (and aquomet Hb) has a unique quaternary structure form which is slightly different from the typical R state of human oxy Hb, the greylag goose oxy Hb and the chicken oxy HbD. We named this the R_H form (Liu *et al.*, 2001) and hypothesize that it must be caused by the mutations between the two goose Hbs. Further studies on other highland bird and animal Hbs are necessary to confirm this hypothesis.

3.3. Speculated roles of the four mutations between greylag goose and bar-headed goose Hbs

3.3.1. Roles of mutations at α119(H2) and β125(H3). In the structure of the bar-headed goose oxy Hb and aquomet Hb the closest distances between Alaα119 and Leuβ55 are 4.56 and 4.52 Å, respectively, which are too great to make a van der Waals contact (Zhang *et al.*, 1996; Liu *et al.*, 2001). In the structure of greylag goose oxy Hb the closest distance between Proα119 and Leuβ55 is 3.79 Å, indicating the presence of a van der Waals contact between the two residues (Fig. 3) and confirming the previous postulation.

In addition to α119(H2), β125(H3) is also located on the $\alpha_1\beta_1$ interface (Liu *et al.*, 2001). In the structure of greylag goose oxy Hb, the side chain of Gluβ125(H3) might form a salt bridge with Hisα50(CD8) at a distance of 3.75 Å if the side-chain flexibility of Glu and His are considered (Fig. 4*b*). In fact, the side chain of Hisα50 may possesses alternative conformations (Fig. 4*a*). In the bar-headed goose oxy Hb (Zhang *et al.*, 1996), the closest distance between Aspβ125 and Hisα50 is 8.23 Å, indicating the absence of contact between the two residues. Although in the bar-headed goose oxy Hb Aspβ125 OG1 makes a van der Waals contact with Thrα34(B14) CG at a distance of 3.49 Å (Zhang *et al.*, 1996), van der Waals interactions are generally weaker than salt bridges. Therefore, the mutation Glu (greylag goose)$\rightarrow\beta$125Asp (bar-headed goose) may also play a partial role in the

higher oxygen affinity of bar-headed goose Hb. Protein-engineering experiments are needed to prove the physiological function of β125.

3.3.2. Roles of mutations at α18(AB) and α63(E14). Residue α18 of greylag goose Hb is Gly. Analysis using *DSSP* (Kabsch & Sander, 1983) indicates that residues α3–15 construct the *A* helix of the Hb. Residues α16–17 are in a turn conformation and α18–20 are in 3_{10}-helix conformation (Fig. 5*a*). In bar-headed goose Hb α18 is Ser. Residues α3–17 construct the *A* helix and residues α18–20 construct the *AB* corner. Compared with greylag goose oxy Hb, the *A* helix of bar-headed goose oxy Hb is elongated by two residues. Therefore, the mutation at α18 causes remarkable conformational changes in main chain α15–22 between the two species. The changes can also be seen in Fig. 2, in which the r.m.s. deviations of residues in main-chain residues α15–22 between the two species are at least two times larger than those of the residues in the BGH fitting frame.

The mutation at α18(B1) affects the conformation of α21. Alaα21 shifts relative to α63(E12) in the direction from the C-terminus to N-terminus of helix *E*. Therefore, the position of the starting residues of the *B* helix also changes relative to the *E* helix where α63 resides (Fig. 5*b*). The strain arising from the position changes of the *AB* corner and the start of helix *B* relative to the helix *E*, together with the larger side chain of Valα63 in bar-headed goose oxy Hb, pushes the *E* helix towards the *EF* corner and induces a series of shifts of the *CD* corner, *F* helix and *FG* corner in the same direction. The α *FG* corner, which is at the 'flexible joint' in the $\alpha_1\beta_2$ interface, is pulled slightly further away from the β_2 subunit and the interactions between residues in the $\alpha_1\beta_2$ interface make the $\alpha_2\beta_2$ dimer rotate 2.8° and translate 0.5 Å relative to the $\alpha_1\beta_1$ dimer in order to maintain the original contacts in the interface, so that there is no remarkable contact change in both the 'flexible joint' and 'switch region' in the $\alpha_1\beta_2$ interface between the two species.

To sum up, although the mutations α18 and α63 are located at the molecular surface, mutation α18 together with mutation α63 significantly change the main-chain conformation of the *AB* corner and finally lead to the difference in quaternary structure between the two species.

As we know, Gly has a unique geometrical future: its conformational angle φ and ψ values are in a wide range, it has the greatest flexibility of the amino-acid residues and often appears in the positions where the peptide chain requires a movement or turning. It is interesting that in most of Hb species with normal or lower oxygen affinity, such as human, greylag goose, Canadian goose, mute swan *etc*., α18 is Gly and α63 is Ala as shown in a BLAST search (Altschul *et*

Table 4
Ligand geometries of the haem in greylag goose and bar-headed goose oxy Hbs.

	Greylag goose oxy Hb		Bar-headed goose oxy Hb	
	α	β	α	β
B factor of Fe (Å^2)	23.58	27.55	23.51	19.83
B factor of O1—O2 (Å^2)	43.18	36.85	30.93	23.65
Fe—O1—O2 angle (°)	145.8	130.3	170.2	158.7
Fe—O1 distance (Å)	1.74	1.75	1.78	1.81
His*F*8 NE2—Fe distance (Å)	2.19	2.14	2.10	2.07
His*E*7 NE2—O2 distance (Å)	2.69	2.55	2.53	2.57
*F*8 NE2—Fe—O1 angle (°)	171.6	171.4	174.9	175.4
Val*E*11 CG2—O2 distance (Å)	3.28	3.40	3.22	3.25
R.m.s. deviation from plane† (Å)	0.103	0.094	0.157	0.120
Fe-to-plane distance (Å)	0.26	0.16	0.211	0.132

† The plane is defined as that passing through all haem atoms excluding the side chains and Fe atom.

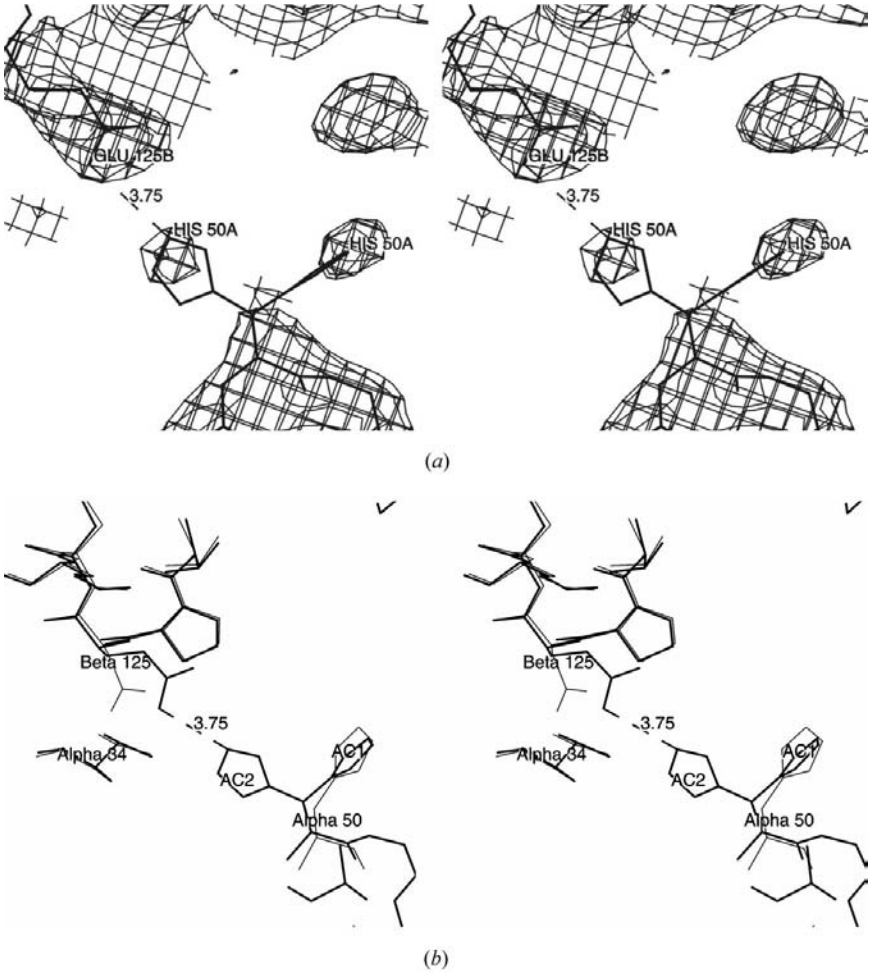

Figure 4
Contact between Gluβ125(H3) and Hisα50(CD8) in greylag goose oxy Hb. (*a*) $2mF_o - DF_c$ electron-density map around residues α50 and β125; two alternative conformations of Hisα50 are shown. (*b*) Structural comparison around Gluβ125 and Hisα50 between greylag goose oxyHb (thick line) and bar-headed goose oxy Hb (thin line).

al., 1997). In fact, the greylag goose, chicken and human oxy Hbs all have similar quaternary structure, while the bar-headed goose oxy Hb has a unique quaternary structure (Liu *et al.*, 2001). The structure of bar-headed goose deoxy Hb also shows a unique quaternary arrangement which is different from that of the typical T state of human deoxy Hb. The unique quaternary structures of both bar-headed goose oxy Hb and deoxy Hb may allow more easy transition between the R and T states than in greylag goose Hb and human Hb (Liang *et al.*, 2001).

3.4. The haem-group region and IPP-binding site

3.4.1. The haem-group region. Fig. 1 shows that the haem group and the residues around it in the greylag goose oxy Hb structure fit well to electron densities. A comparison of the geometries around the haem group between the greylag goose oxy Hb and the bar-headed goose oxy Hb is given in Table 4. There is no residue difference in the haem-group region of the two goose Hbs, so that the geometries around the haem group of the two species are similar except that the group *B* factors of Fe and O_2 of the greylag goose oxy Hb are obviously larger than those of the bar-headed goose oxy Hb and its Fe—O1—O2 angle is smaller. These differences may mainly be caused by the lower resolution of the greylag goose oxy Hb structure.

3.4.2. The IPP-binding site. Inositol 1,3,4,5,6-pentaphosphate (IPP) is the organic phosphate allosteric effector for avian Hbs (Isaacks & Harkness, 1980). It binds to the human Hb at the entrance to the central cavity between the N- and C-termini of the two β-subunits (Arnone, 1972; Perutz, 1983). The level of IPP is the same in the red blood cells of greylag goose and bar-headed goose and both the bird Hbs show the same affinity for IPP (Rollema & Bauer, 1979).

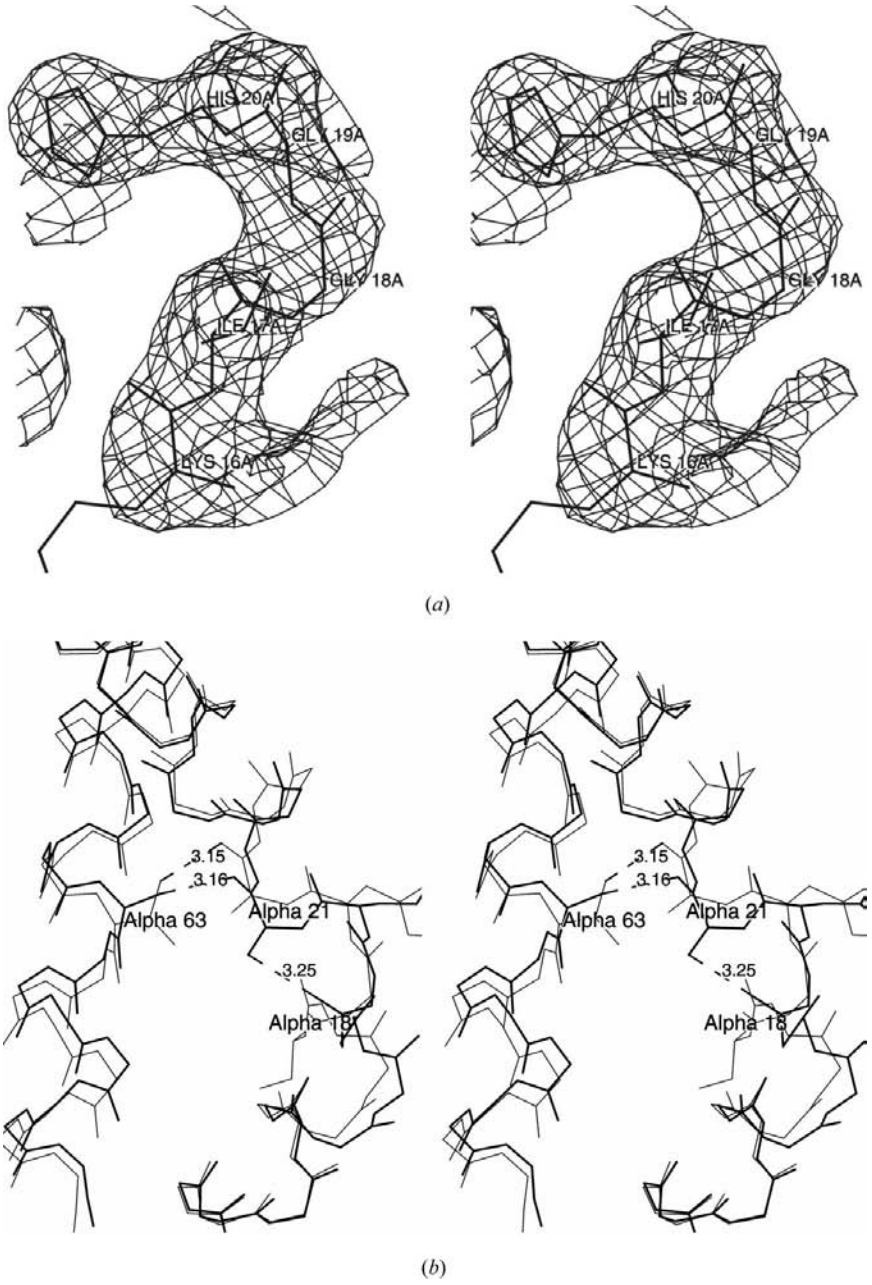

Figure 5
The conformational differences between greylag goose (thick line) and bar-headed goose (thin line) oxy Hbs arising from the mutations at α18 and α63. (*a*) $2mF_o - DF_c$ electron-density map around the residues from α16 to α20; (*b*) the conformational differences around the α18 and α63 mutation sites between the two species.

The IPP-binding site of the greylag goose and bar-headed goose Hbs may involve the same residues, including Valβ1, Hisβ2, Lysβ82, Argβ104, Argβ135, Hisβ139, Argβ143, Lysβ144 and Hisβ146 of both the β_1 and β_2 subunits, which form a positively charged environment; of these residues, Hisβ2 and Argβ104 may be too distant to interact directly with IPP. The main chains of residues β135–146 of both β-subunits construct the entrance to the central cavity of the Hb molecule and the positively charged side chains mentioned above bond to the negatively charged IPP. Nevertheless, the IPP-binding sites of greylag goose and bar-headed goose oxy Hbs show slightly different features arising from the changes in their quaternary structures.

4. Discussion

Although the crystal structure of the greylag goose oxy Hb is at the lower resolution of 3.09 Å, the final structure is reliable

with the low R and R_{free} values and small error values and the key regions such as haem pockets, the four mutated residues and the IPP-binding site fit well to the electron-density map. It is perfectly reasonable for us to compare the overall changes in quaternary arrangements and main chains of the Hbs. The structure supports Perutz and Bauer's conclusion that the mutation Proα119Ala produces a two-carbon gap between α119 and β55 in bar-headed goose Hb which is absent in greylag goose Hb. Proα119Ala is responsible for the higher oxygen affinity of bar-headed goose Hb, as there is evidence that either Proα119Ala or Metβ55Ser mutation of human Hb increases the oxygen affinity. In addition, the roles of the other three mutations between the two species are also analyzed. Our conclusions are that the mutation Gluβ125Asp might also contribute to the higher oxygen affinity to some extent, in addition to Proα119Ala; the mutations Glyα18Ser and Alaα63Val are responsible for the unique quaternary structures of both the oxy and deoxy forms of bar-headed goose Hb, which might be responsible for its unique allosteric mechanism (Liang *et al.*, 2001); the two mutations might therefore not be functionally neutral, although they may not be responsible for higher oxygen affinity.

From an evolutionary point of view, it is interesting to note that only one or a few mutations will change the protein conformation and its biological function. Perutz has previously pointed out that the altered properties of some animal Hbs can be attributed to one or a few mutations (Perutz, 1983), although their effects may be dramatic or subtle, which is consistent with the neutral theory of molecular evolution (Kimura, 1979). The bar-headed goose and greylag goose Hbs are the best examples in nature. Many other natural mutation examples of avian Hbs show that a raised blood oxygen affinity is advantageous for birds living at high altitudes and it is one or a few mutations that play the crucial role in the evolutionary process (Liu *et al.*, 2001).

We would like to thank Professor Ru-chang Bi of the Institute of Biophysics, Academia Sinica for his help in data collection. The project was supported by the National Natural Science Foundation of China.

References

Acqua, W. D., Goldman, E. R., Lin, W., Teng, C., Tsuchiya, D., Li, H., Ysern, X., Braden, B. C., Li, Y., Smith-Gill, S. J. & Mariuzza, R. A. (1998). *Biochemistry*, **37**, 7981–7991.
Altschul, S. F., Madden, T. L., Schäffer, A. A., Zhang, J., Zhang, Z., Miller, M. & Lipman, D. J. (1997). *Nucleic Acids Res.* **25**, 3389–3402.
Arnone, A. (1972). *Nature (London)*, **237**, 146–149.
Baldwin, J. M. & Chothia, C. (1979). *J. Mol. Biol.* **129**, 175–220.
Black, C. P. & Tenny, S. M. (1980). *Respir. Physiol.* **39**, 217–239.
Braunitzer, G. & Oberthur, W. (1979). *Hoppe-Seyler's Z. Physiol. Chem.* **360**, 679–683.
Brünger, A. T. (1992). *X-PLOR Version 3.1. A System for X-ray Crystallography and NMR.* New Haven: Yale University Press.
Brunger, A. T., Adams, P. D., Clore, G. M., DeLano, W. L., Gros, P., Grosse-Kunstleve, R. W., Jiang, J. S., Kuszewski, J., Nilges, M., Pannu, N. S., Read, R. J., Rice, L. M., Simonson, T. & Warren, G. L. (1998). *Acta Cryst.* D**54**, 905–921.
Collaborative Computational Project, Number 4 (1994). *Acta Cryst.* D**50**, 760–763.
Fermi, G. & Perutz, M. F. (1981). *Haemoglobin and Myoglobin*, edited by D. C. Phillips & F. M. Richards, pp. 10–11, 66–67. Oxford: Clarendon.
Hiebl, I., Braunitzer, G. & Schneeganss, D. (1987). *Biol. Chem. Hoppe-Seyler*, **368**, 1559–1569.
Howard, A. J., Nielsen, C. & Xuong, N. H. (1987). *Methods Enzymol.* **114**, 452–472.
Isaacks, R. E. & Harkness, D. R. (1980). *Am. Zool.* **20**, 115–129.
Jessen, T. H., Weber, R. E., Tame, J. & Braunitzer, G. (1991). *Proc. Natl Acad. Sci. USA*, **88**, 6519–6522.
Kabsch, W. & Sander, C. (1983). *Biopolymers*, **22**, 2577–2637.
Kimura, M. (1979). *Sci. Am.* **241**, 94–104.
Knapp, J. E., Oliveira, M. A., Xie, Q., Erust, S. R., Riggs, A. F. & Hacker, M. L. (1999). *J. Biol. Chem.* **274**, 6411–6420.
Laskowski, R. A., MacArthur, M. W., Moss, D. S. & Thornton, J. M. (1993). *J. Appl. Cryst.* **26**, 283–291.
Liang, Y. H., Hua, Z. Q., Liang, X., Xu, Q. & Lu, G. Y. (2001). *J. Mol. Biol.* **313** 123–137.
Liu, X. Z., Li, S. L., Jing, H., Liang, Y. H., Hua, Z. Q. & Lu, G. Y. (2001). *Acta Cryst.* D**57**, 775–783.
Luzzati, V. (1952). *Acta Cryst.* **5**, 802–810.
McRee, D. E. (1992). *J. Mol. Graph.* **10**, 44–46.
Oberthur, W., Braunitzer, G. & Wurdinger, I. (1982). *Hoppe-Seyler's Z. Physiol. Chem.* **363**, 581–590.
Oberthur, W., Voelter, W. & Braunitzer, G. (1980). *Hoppe-Seyler's Z. Physiol. Chem.* **361**, 969–975.
Perutz, M. F. (1983). *Mol. Biol. Evol.* **1**, 2–28.
Perutz, M. F., Fermi, G., Luise, B., Shaanan, B. & Liddington, R. C. (1987). *Acc. Chem. Res.* **20**, 309–321.
Petschow, D., Wuerdinger, I., Baumann, R., Duhm, J., Braunitzer, G. & Bauer, C. (1977). *J. Appl. Physiol.* **42**, 139–143.
Rollema, H. S. & Bauer, C. (1979). *J. Biol. Chem.* **254**, 12038–12043.
Swan, L. W. (1970). *Nat. Hist.* **79**, 68–75.
Weber, R. E., Jessen, T. H., Malte, H. & Tame, J. (1993). *J. Appl. Physiol.* **75**, 2646–2655.
Zhang, J., Hua, Z. Q., Tame, J., Lu, G. Y., Zhang, R. J. & Gu, X. C. (1996). *J. Mol. Biol.* **255**, 484–493.